Asociación Argentina
de Mecánica Computacional

Mecánica Computacional Vol XXXIII, págs. 1767-1781 (artículo completo)
Graciela Bertolino, Mariano Cantero, Mario Storti y Federico Teruel (Eds.)
San Carlos de Bariloche, 23-26 Setiembre 2014

ROBUST IDENTIFICATION AND PASSIVE CONTROL OF VIBRATION OF A TEST RIG UNDER UNCERTAIN CONDITIONS

Cesar A. da Fonseca, Roberta Lima, Gustavo B. Wagner and Rubens Sampaio

Pontifícia Universidade Católica do Rio de Janeiro, Rua Marquês de São Vicente, 225 Gávea, RJ, CEP: 22453-900, Brazil Rio de Janeiro

Keywords: Robust identification, Passive control, Nonlinear dynamic absorber

Abstract. A continuous dynamical system under vibratory excitation may display several resonance situations. Therefore, a vibration absorber attached to the mechanical device can be quite important, especially when a projected operation point causes high vibration amplitudes. Health of equipment is also a main concern, or human comfort, when there is people near a machine the use of an absorber is a common solution in structure and machine dynamics. Ordinary vibration absorbers are designed as an additional degree of freedom that, theoretically, completely stops one of the other elements to vibrate at a specified frequency. So, in order to prevent more than one critical point, one may need to add the same number of absorbers as the number of harmful resonances. Also, each time you cancel one resonance frequency, the mechanical system increases in the same proportion the number of degrees of freedom. This work proposes to analyze theoretically and simulate a nonlinear absorber, which is capable to diminish the vibrations at more than one resonance frequency. It will be shown through simulations how the variation of the absorber parameters can modify the response of the system. Then, a stochastic modeling is also done to account for the applied force of the system that is considered a random process to test the efficiency of the nonlinear absorber. Further, an experimental set up will be presented that models a two-floor building with an ordinary absorber and also with a new concept of a non-linear absorber. The new absorber is assembled with two thin blades connecting a mass allowed to move only in one direction. Test data will be collected by accelerometers and the test rig is excited by a shaker for robust identification and to validate the model used in the simulation. The attached nonlinear absorber shall then reduce the vibration when an unbalanced rotor turning at variable speed is the source of perturbation.

1 INTRODUCTION

To model a structure it is important for any engineer who wants to do a vibrational analysis on it. Usually one desires low vibration amplitudes at a specific frequency or several frequencies. Therefore, it may be necessary to reduce the oscillation amplitudes to accepted levels, which may be achieved by adding a new element to the structure, an absorber. In its simplest form it can be modeled as a mass-spring system, hence with only one parameter, its natural frequency. An absorber design can be found in undergraduate vibration textbooks Den Hartog (1956) and Inman (2007). Theoretically, a linear absorber can eliminate the vibration for only one specific forcing frequency and for one of the degrees of freedom. Although, this is not enough if one desires that more than one degree of freedom have low amplitudes. In this cases, it is necessary to add more linear absorbers what is a complicate procedure.

There are recent new studies showing that a nonlinear approach like adding nonlinear elastic elements can reduce significantly the oscillations at more than one frequency and for more than one degree of freedom. The work of Bellizzi and Pinhede (2013) has shown experimentally that adding these nonlinear elements at the end of a cantilever beam has reduced its oscillatory displacements. The nonlinear absorber can also be seen as a mean to pump energy out of a system as in Kerschen G.; Vakakis and Bergman (2005) who conducted numerical and experimental studies. Other articles from Starosvetsky and Gendelman (2009) and Gendelman and Feldman (2008) have demonstrated through numerical studies that nonlinear absorber act as energy sinks and have also shown the coexistence of attractors in their dynamics. An example of how a nonlinear mechanism has a force proportional to the cubic of its displacement is found in Kovacic and Brennan (2011). More recent, and more advanced, works regarding the linear absorber were done by S. and Høgsberg (2014), where the proper tuning of an absorber for continuous flexible structures is discussed.

The present work develops a stochastic approach to a two-degree-of-freedom model inspired on a test rig built at PUC-Rio, which is modeled here by two masses connected by two linear springs. The system is excited by a harmonic force at the first mass using an unbalanced motor. A linear absorber was built and assembled to the structure and with this setting it was possible to lower the amplitude vibration when the forcing frequency was set to excite the system at any of its two resonance frequencies. The goal of this work is to analyze the behavior of the structure when a linear absorber is replaced by a nonlinear one and how this new type of absorber can be built and mounted to the original structure. Of course, when a nonlinear absorber is coupled to the system it is no longer possible to determine analytically the amplitude of the response to a harmonic force; one has to approximate the response numerically. Consequently, the first study that was done is to search for the best design of a nonlinear absorber, which is capable to reduce significantly vibration on the coupled structure (test rig with absorber). Secondly, since the test rig is constantly modified and its properties determination become imprecise, a stochastic model was also made to verify the robustness of the results. Moreover, the stochastic study is important to test the sensibility of the nonlinear absorber elastic property and its capacity to reduce the vibrations.

In section 2, the model of the test rig as a two-body system and a model of the nonlinear absorber will be described. In the section 4, the deterministic analysis and its results are displayed showing the numerical efficiency of the nonlinear absorber and an assembly scheme of how a nonlinear absorber could be built. Next, in sections 5 and 6, a stochastic study is shown, in which a characteristic of the of the excitation force that acts on test rig/system is considered random and modeled as a random process. The conclusions, comparison between the results of

the deterministic and stochastic simulations, are in the last section.

2 DETERMINISTIC MODEL OF THE SYSTEM

2.1 Description of the test rig

The experimental test rig consists of two platforms, one on the top of the other. The first one is fixed to the ground with four thin steel blades and the second is attached to the first platform by others four blades, the blades will be modeled as beams. A DC-motor driving an unbalanced disc is placed on the first platform and when the disk is turning at a fixed rotation it induces a harmonic force on the system. Figure 1 shows how the test rig is assembled and where the DC-motor and disk are placed.

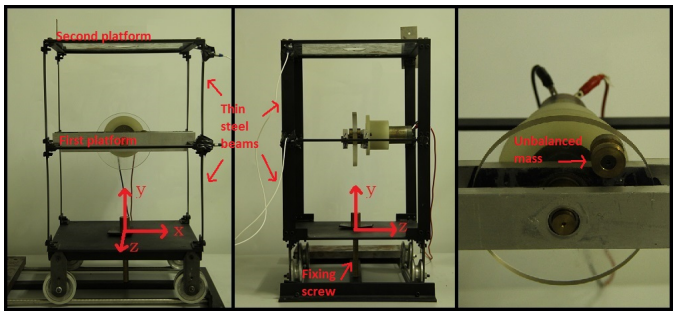

Figure 1: The test rig assembly. On the left, two platforms are assembled with thin steel blades. In the middle, it is shown how the first platform is fixed to the ground. On the right, the DC-motor is shown with the unbalanced disk.

At the top, one more element is added, the absorber, with the objective to reduce the vibrations induced by the motor-unbalanced disk. At first, a linear absorber is attached to the top. It is capable to eliminate all the vibration at least at one platform for one specified excitation frequency. But, since we desire to reduce the vibrations in the two platforms, a nonlinear absorber, instead of a linear one, will be used. As will be seen it is able to lower significantly the amplitude in the two platforms for a bandwidth of frequencies near the resonances of the linear system. One of the problems addressed here is how to construct the nonlinear absorber, say a spring with cubic behavior.

The nonlinear absorber can be realized with two identical thin steel blades that are joined by a connecting part placed in the middle with motion restricted to a line segment in a direction perpendicular to the steel blades in the equilibrium configuration. A track assures this restriction is realized. The whole set up is built inside a light box and placed on the top of the second platform of the structure. Other assemblies can be done, as for example replacing the blades for steel strings or, also, by compressing the blades, which will significantly increase the nonlinear behavior of the absorber, because in this case the system would have two symmetric stable positions. Both situations will not be dealt with in the present study and are left for a future work.

Experimental data was acquired using accelerometers placed at two points of the structure, one in each platform. The sensors generate a voltage signals linearly depended of the acceleration, that are analyzed and displayed by an oscilloscope. The motor terminals are connected to DC-power source, which is manually operated. By varying the input voltage, the motor drives an unbalanced disc and causes vibrations of the test rig. It was visually observed that the forcing frequencies in which the platforms have maximum oscillation amplitudes, are around 3.0

Hz and around 7.5 Hz. Then, using an impact hammer we could transform the temporal signals to the frequency domain in order to determine the spectrum of frequency.

2.2 Mathematical model of the test rig

The test rig is sketched as seen in figure 2, and is modeled as a two-degree-of-freedom system. Each of them represents the displacement of one platform of the test rig. It is a rather simple and rough model, but is enough to show the validity of the absorber and for preliminary studies. Other effects will not be taken into account, as for example the rotational movement of the structure.

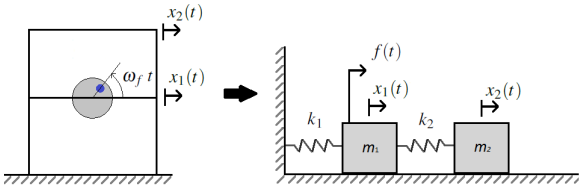

Figure 2: The structure model as a two spring-mass elements.

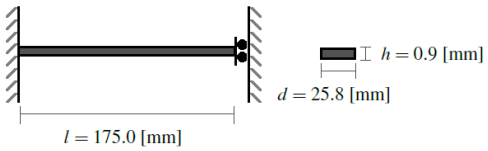

Figure 3: Modeling the steel beams.

Due to the test rig configuration, each steel blade of the system is considered to be a beam with fixed-free boundary conditions and with no angular displacement at the end plane section to compute the equivalent stiffness. So, it is assumed that each beam behaves as a linear spring with an equivalent stiffness, k_{beam}, calculated by Inman (2007).

$$k_{beam} = 12\frac{EI}{l^3}, \tag{1}$$

where E is the elastic modulus of steel, I is the moment of area of the cross-section of the blade and l is the blade length. In the two-degree-of-freedom model, each spring (k_1 and k_2) represents a group of four parallel steel blades, thus each elastic constant is calculated as: $k_1 = k_2 = 4\ k_{beam}$.

Calling x_1 and x_2 the displacements of the platforms, m_1 and m_2 its masses and k_1 and k_2 the equivalent stiffness of each group of four steel blades. And $f(t)$ is an harmonic force exciting the first degree of freedom.

2.3 Mathematical model of the nonlinear absorber

If one desires that there is no vibration at one of the masses for a given forcing frequency, he will necessarily couple a new spring-mass element, whose natural frequency matches the specific frequency that reduces the vibration. Numerically, it means to adjust the values of the stiffness and the mass of the absorber in the transfer function equation of motion to set a *zero* for a specific frequency. Therefore, the linear absorber will only work for one forcing frequency. The purpose of this work is to establish a new type of absorber capable to reduce the vibration for a bandwidth of frequencies.

As described in the introduction, the coupling of a nonlinear absorber element to the two-degree-of-freedom system makes it possible to diminish the vibration amplitudes wider range than just one frequency for a linear absorber. Likewise, the nonlinear absorber we chose to work with is an additional degree of freedom but its elastic force is proportional to the cubic of the displacement. In order to obtain this elastic nonlinear force, two linear springs and a restrained mass, see figure 4, can derive into an elastic cubic relationship to the displacement of the mass.

The formulation begins with two linear springs and one mass, which is restrained to move only

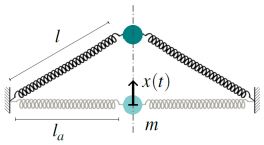

Figure 4: A type of non-linear absorber.

vertically when the springs are at rest, as in figure 4. The vertical components of the elastic forces lead the following differential equations:

$$m\ddot{x} + 2k\left(\sqrt{l_a^2 + x^2} - l_n\right)\frac{x}{\sqrt{l_a^2 + x^2}} = 0, \quad m\ddot{x} + 2k\left(x - \frac{l_n x}{\sqrt{l_a^2 + x^2}}\right) = 0, \tag{2}$$

where one can approximate the square root with a Taylor expansion and, regarding only the first term, the cubic proportionality appears.

$$\left(\sqrt{l_a^2 + x^2}\right)^{-1} = l_a\sqrt{1 + \left(\frac{x}{l_a}\right)^2} \approx 1 - \frac{1}{2}\left(\frac{x}{l_a}\right)^2 + \frac{3}{8}\left(\frac{x}{l_a}\right)^4 - \cdots, \tag{3}$$

And it becomes

$$m\ddot{x} + 2k\left(1 - \frac{l_n}{l_a}\right)x + k\frac{l_n}{l_a^3}x^3 = 0. \tag{4}$$

The equation (4) is the dynamical equation of the nonlinear absorber involving a cubic relationship regarding the displacement of x. We define a nonlinear constant γ and we could choose the geometric parameters l_a, equal to the dynamical one l_n to eliminate the linear term and the spring force is then purely cubic:

$$\ddot{x} + \gamma x^3 = 0, \qquad \gamma = \frac{k}{ml_a^2}. \tag{5}$$

2.4 The structure model with the nonlinear absorber

So we write the dynamic model with one nonlinear elastic term. While considering equation (4) as a new element to the model. The new model is sketched in figure 5 where the coordinate x from eq. (5) is substituted by the relationship $x = x_3 - x_2$, $k = k_3$ and $m = m_3$.

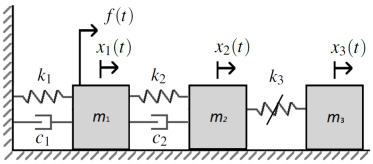

Figure 5: New three degree of freedom system with the nonlinear absorber coupled.

$$[m]\{\ddot{x}(t)\} + [c]\{x(t)\} + [k]\{x(t)\} = \{f(t)\} + \{f_{nl}(t)\}, \tag{6}$$

where $[m]$ and $[c]$ are matrices and $[k]$ and the nonlinear term f_{nl} are written:

$$[k] = \begin{pmatrix} k_1 + k_2 & -k_2 & 0 \\ -k_2 & k_2 + 2k_3(1 - l_n/l_a) & -2k_3(1 - l_n/l_a) \\ 0 & -2k_3\,(1 - l_n/l_a) & 2k_3(1 - l_n/l_a) \end{pmatrix}. \tag{7}$$

$$\{f_{nl}(t)\} = \begin{pmatrix} 0 \\ k_3 \dfrac{l_n}{l_a^3}\left[x_3(t) - x_2(t)\right]^3 \\ -k_3 \dfrac{l_n}{l_a^3}\left[x_3(t) - x_2(t)\right]^3 \end{pmatrix}. \tag{8}$$

2.5 The design of the nonlinear absorber

A nonlinear absorber can be constructed in several different ways. Some authors use membranes, others steel strings, but we decided to work with the same material used to build the test rig and our *Ansatz* to realize the nonlinear absorber is given by eq. (5). The absorber concept is shown below in fig. 6. The absorber consists of a mass, as is represent by the block in the

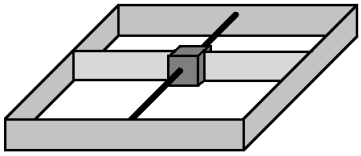

Figure 6: Concept of the nonlinear absorber.

middle, and by two thin steel blades similar to the columns of the test rig and a square box. The springs are assembled in such a way that they are force-free when the block is at the equilibrium point. The black rod which crosses the block works as a rail, so that the block would not move nor rotate in any other direction. The square box is screwed to the top of the structure on the second platform. Therefore it is coupled to the second platform and shall move in only one direction and it is easily dismounted.

3 PARAMETER DETERMINATION OF THE TEST RIG

As mentioned before, the test rig was instrumented with several attached accelerometers. Two were placed at the platform pointing at the direction of more movement and one was built orthogonally to them. The presence of the third sensor is intended to validate the plane-two-degree-of-freedom model shown in section 2. Since no relevant output was measured in relation to the others accelerometers, any other phenomenon such as structural twist or vertical vibration can be disregarded in the range of our analysis. The parameters intended to be acquired are the natural frequencies of the system and its damping factors, or ω_1, ω_1, ζ_1 and ζ_2, respectively. Also the modes u_1 and u_2 are parameters to be acquired.

In figure 8 it is possible to see the impact signal analysis. The two top graphs show the accelerometer response on the first and second platform, when an impact hammer was used to excite only the first platform. The two bottom below are the same response, but the impact hammer hit the second platform. The peaks match the first and second natural frequencies observed manually in all cases. The natural frequencies are $\omega_1 = 3.23$ Hz $\omega_2 = 7.75$ Hz.

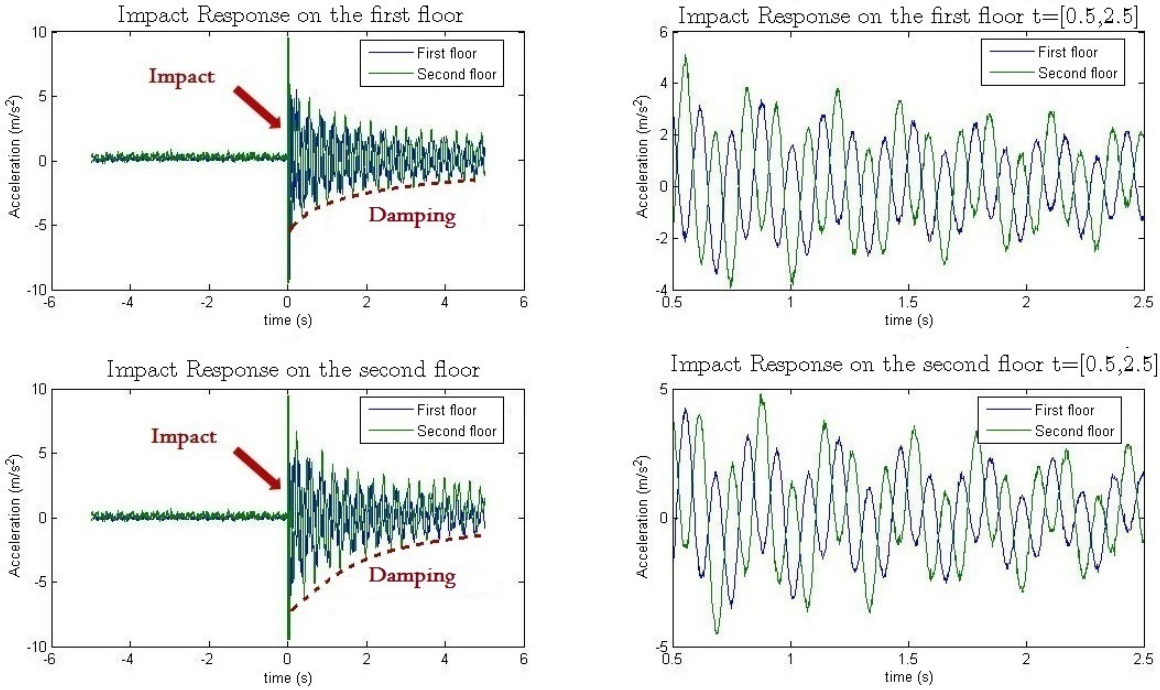

Figure 7: Time domain acquisition from test rig showing the impact at $t = 0$s.

The corresponding frequency modes were calculated using a DSLR camera pointing the structure taking multiple shot from it. With help from an image editing software it, the relationship between the displacements of the degrees of freedom could be stipulated, see figure 9 below.

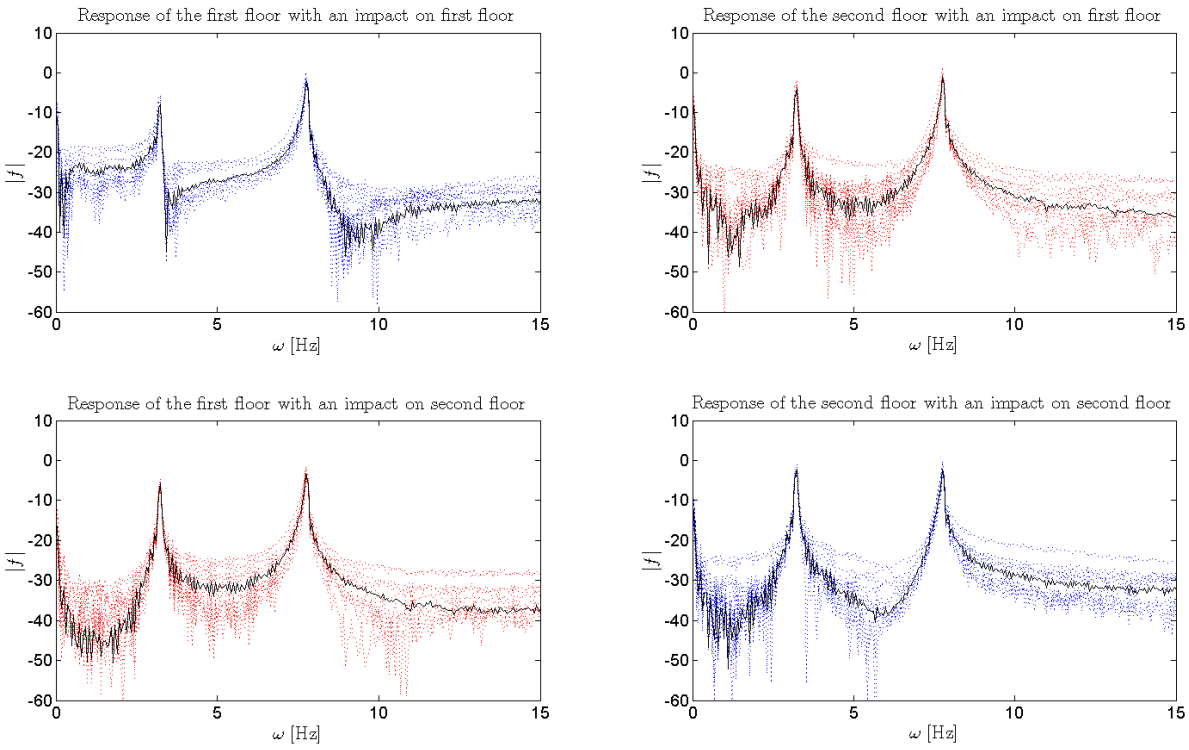

Figure 8: FFT impact acquisition from test rig.

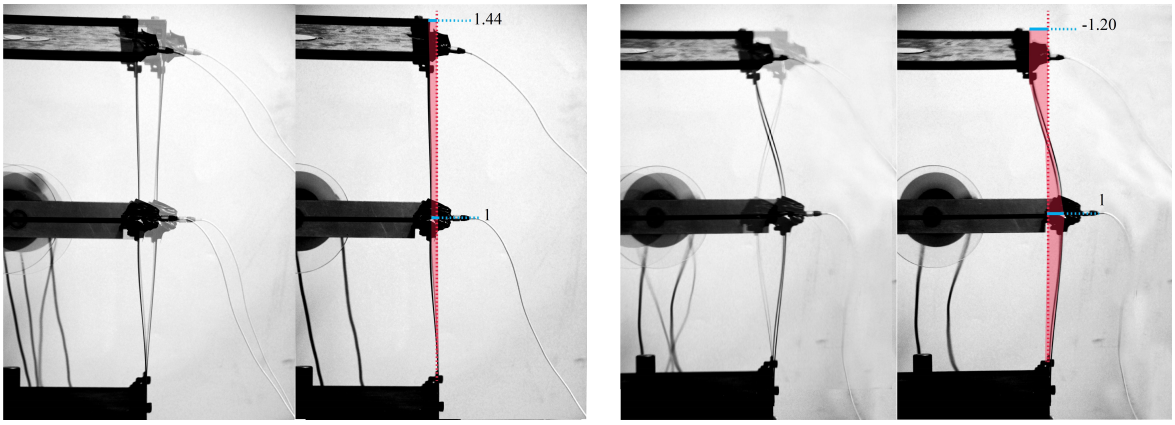

(a) (b)

Figure 9: First vibration mode, 3.23 Hz(a). Second vibration mode, 7.75 Hz(b).

$$\text{First Mode } u_1(t) = \begin{pmatrix} 1 \\ 1.44 \end{pmatrix}, \qquad \text{Second Mode } u_2(t) = \begin{pmatrix} 1 \\ -1.20 \end{pmatrix} \tag{9}$$

Moreover, by setting the motor to excite at the forcing frequency at one of the natural frequencies, the ratio between all collected points of acceleration during a desired time was calculated and its mean obtained. Then, with one peak sample as amplitude and with the forcing frequency value, we could plot two functions in time at the same mean ratio. In Figure 10, both functions and the acquisition in both natural frequencies are plotted. It shows a good validation from eigenvectors (9) determined with the camera although the high noise interference.

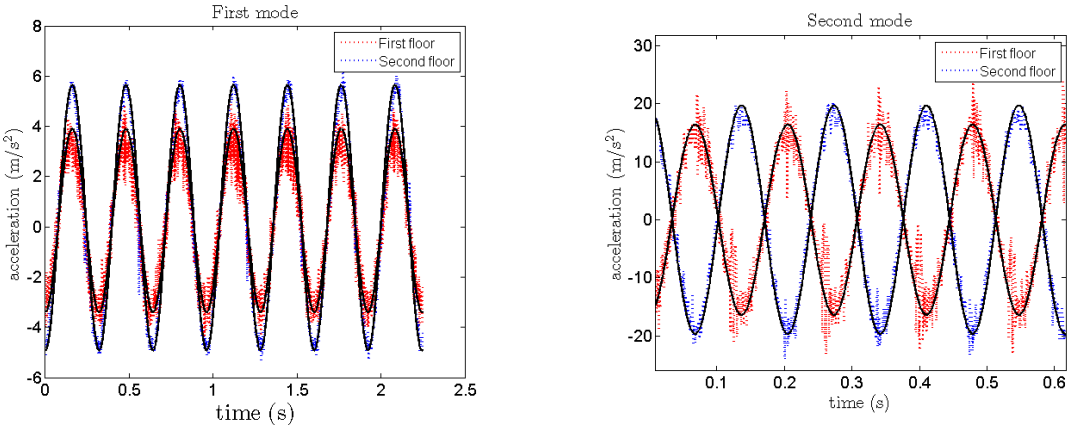

(a) (b)

Figure 10: First vibration mode, 3.23 Hz(a). Second vibration mode, 7.75 Hz(b).

The final parameter to be discovered is the damping of the system. The proper method in finding it was setting the motor again at the natural frequencies for a certain time, in order that all transients and other disturbance settle. Then, the motor power source is suddenly cut off and the whole system remains vibrating at its modal shape, but each amplitude gets lower each cycle. Then the logarithmic decay formula enable us to calculate the damping factors by counting the difference between the peaks. Equation 10 solve the values for the damping factors.

$$\delta = \frac{1}{N}\left(\frac{x_k}{x_{k+N}}\right) = \frac{2\pi\zeta}{\sqrt{1-\zeta^2}}, \tag{10}$$

where N is the number of cycles between the peaks x_k and x_{k+N}. Two test were conducted and both showed qualitative the same number. The modal damping factors are respectively $\zeta_1 = 0.012$ and $\zeta_2 = 0.006$. With all the parameter determined, it is possible to mount the complete model with masses and stiffness values using the eigenvector matrix.

4 SIMULATIONS OF THE DETERMINISTIC SYSTEM

In all deterministic and stochastic simulations, eq. (6) was integrated in a range of [0.0, 20.0] seconds considering that each coordinate x_1, x_2 and x_3 has null initial conditions to position and to velocity. For the integrations, it was used the function *ode45* (based on the Runge-Kutta 4th/5th-order method with a varying time-step algorithm) of the *Matlab* software with a maximal steep size equal to 10^{-4} seconds. Also, the maximal absolute error allowed in the integrations was 10^{-4}.

We start analyzing the deterministic model of the structure alone. The structure's parameters, see table 1, and the absorber constant will be considered constant as well as the harmonic force amplitude f_0. The absorber geometric terms l_a and the dynamical l_n will be chosen equal in order to eliminate the linear term of the absorber as shown in eq. (4). Before considering

Parameter	Value	Parameter	Value	Parameter	Value
m_1	2.5 kg	k_1	2800 N/m	c_1	0.5 Ns/m
m_2	1.5 kg	k_2	2800 N/m	c_2	0.5 Ns/m
m_3	0.5 kg	k_3	2800 N/m	f_0	10.0 N
l_a	0.5 m	l_n	0.5 m		

Table 1: Parameters of the system.

analyzing the influence of the absorber, the system natural frequencies of the structure must be known, so that these frequencies will be tested and compared later when the nonlinear absorber is coupled. The natural frequencies were determined by the eigenvalues of the stiffness matrix multiplied by the inverse inertia matrix and are ω_1 = 24 rad/s (3.8 Hz) and $\omega_2 = 59$ rad/s (9.4 Hz), close enough to the natural frequencies of the test rig to test to test the efficiency of the nonlinear absorber, figure 8.

The displacements of the degrees of freedom were simulated setting the forcing frequency ω_f the same as the natural frequencies. The response in time is shown in figure 11, where the two-degree of freedom model was simulated with the dynamical, and in figure 12, where the nonlinear absorber is attached to structure, and whose dynamical equation is eq. (6).

When the system is forced in its natural frequency in the first case, the displacement oscillate higher and higher as expected during resonance, as shown in figure 11. But in the second case, where the model containing the nonlinear absorber was coupled, the results show that the absorber reduces the vibration of the others two coordinates simultaneously for both resonance states. Moreover the absorber moves only a tenth of the displacement of the other coordinates.

In fig. 11 and 12, the capacity of reduction the amplitude of oscillations to both degree of freedom, x_1 and x_2, was observed to the cases of $\omega_f = \omega_1$ and $\omega_f = \omega_2$. But, as explained in the introduction, the nonlinear absorber can reduce significantly the amplitude of oscillations not only at specific frequencies. It can reduce at a bandwidth of forcing frequencies. To verify, this capacity, the system with and without the nonlinear absorber was excited with different ω_f. For each frequency, the models with and without absorber were integrated in a range of [0.0, 10.0] seconds and the maximum displacement of x_1 and x_2 reached during this interval of time (noted

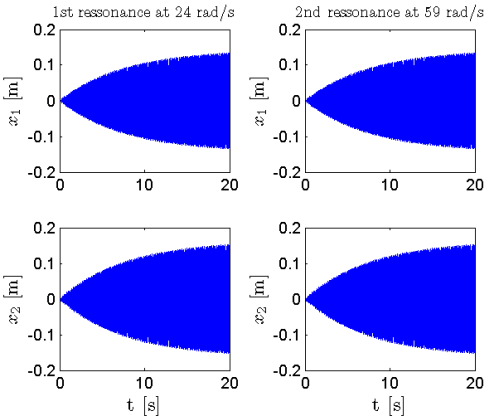

Figure 11: Displacements with an harmonic force at the first and second resonance ω_1 and ω_2 using.

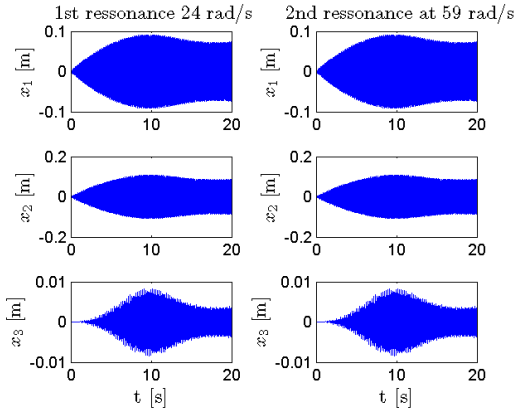

Figure 12: Displacements with an harmonic force at the first and second resonance ω_1 and ω_2 using eq. (6).

as $x_1^\star$ and $x_2^\star$) were computed.

Fig. 13 shows $x_1^\star$ and $x_2^\star$ for forcing frequencies in the bandwidth [0.4, 12] [Hz]. The black marks represent the simulations of the system without the nonlinear absorber, and the red marks with it, eq. (6). Comparing them, it is possible verify that the coupling of the nonlinear absorber reduces the amplitude of oscillation in all bandwidth frequency.

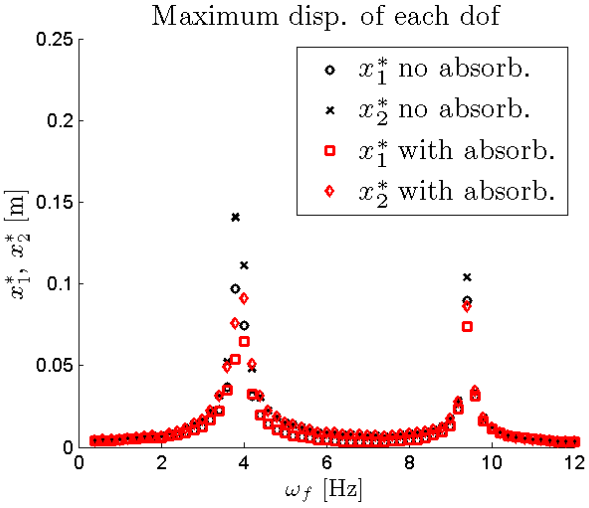

Figure 13: Maximum displacement of the system of a bandwidth analysis.

To observe the influence of the parameter $\gamma = k_3/(m_3 l_a^2)$, eq. (5), in the reduction of the maximum displacements, for different values of this parameter, the system was excited with forcing frequencies, ω_f, in the bandwidth [0.4, 12.0] [Hz]. For each value of γ, a graph similar to the graph shown in fig. 13 was construct and the maximum obtained to $x_1^\star$ and $x_2^\star$(noted as $x_1^{\star\star}$ and $x_2^{\star\star}$) were computed. Figure 14 shows the obtained results, that is, $x_1^{\star\star}$ and $x_2^{\star\star}$ to different values of γ.

It is clear that for bigger values of γ the less the other elements oscillates. In figure 15 the same analysis is presented, but in terms of the percentage of reduction of the vibration amplitude relative to case without the absorber (that is, $\gamma = 0.0$ [1/m^{2}s^2]). One may see that it is possible to have good reductions, up to 50% with γ around 2.5×10^4 [1/m^{2}s^2].

Another interesting result that can be observed is the frequency, ω_f, in which the maximum

value of $x_1^\star$ and $x_2^\star$ (that is, $x_1^{\star\star}$ and $x_2^{\star\star}$) occur as function of γ. Looking at these frequencies, shown in fig. 16, it is possible verify that they could be classified in two groups. One group of frequencies around ω_1 (the first frequency of resonance of the system without the nonlinear absorber), and another group around ω_2 (the second frequency of resonance of the system without the nonlinear absorber).

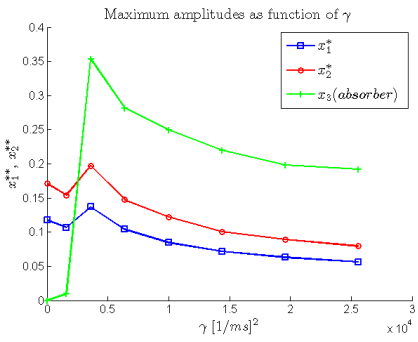

Figure 14: The displacements of the system for different values of γ.

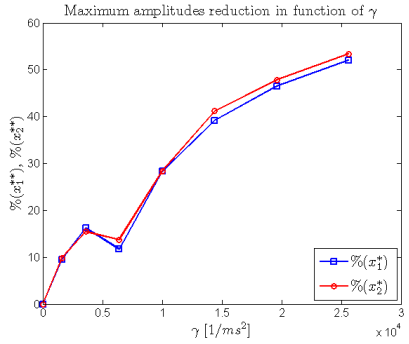

Figure 15: The displacements of the system for different values of γ in percentage.

Another interesting result is the change of the argument of the forcing frequency, or, in other words, where, at which forcing frequency of the bandwidth, the maximum value of the oscillation occur as function of γ. This is shown in figure 16, where one may observe that there is a "jump" of the maximum values of coordinate $x_1^\star$ for γ bigger than 6.0x10^5 1/m^{2}s^2. This happens, because the modeled absorber showed to be more effective to reduce vibration when the forcing frequency matches the first than the second natural frequency. Although, if the nonlinear constant γ increases further than 16x10^5 1/m^{2}s^2, the maximum amplitudes for both coordinates occur again when the forcing frequency is equal to ω_1.

To help visualize the rate of change of the maximum values, $x_1^\star$ and $x_2^\star$ are plotted as function of the forcing frequency and of γ in figure 17.

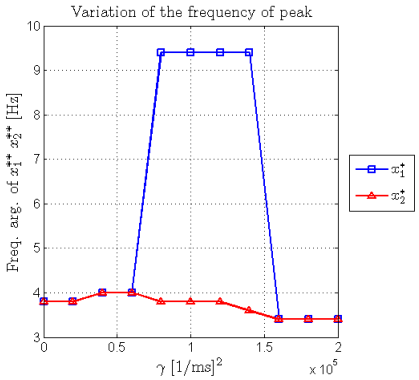

Figure 16: The variation the frequency with highest vibration displacements in terms of γ.

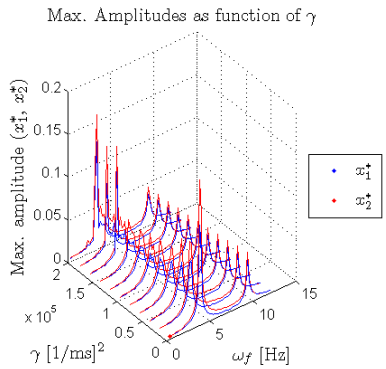

Figure 17: A bandwidth analysis and as function of γ.

5 STOCHASTIC MODEL OF THE SYSTEM

To make a stochastic analysis of the absorber system, it is assumed that the amplitude of the external force is a random process with parameter t constant by parts, represented by $\mathcal{F}_0$. Thus,

we define $\mathcal{F}_0$ as a finite collection of real-valued random variables $\{F_0^1,\ F_0^2, \ldots,\ F_0^n, \ldots\}$, $\forall n \in \mathbb{N}$, from a probability space $(\Omega,\ \mathcal{A},\ P)$, where Ω is the sample space, $\mathcal{A}$ is the σ-algebra and P is the probability measure.

As it is assumed that $\mathcal{F}_0$ is random process constant by parts, given a time-interval with size T, $\mathcal{F}_0(t) = F_0^n$ if $t \in [(n-1)T,\ nT]$, $\quad \forall n \in \mathbb{N}$. Besides this, it is assumed that $\{F_0^1,\ F_0^2, \ldots,\ F_0^n, \ldots\}$ is a collection of equal and discrete random variables, in which each F_0^n, can have only the values f_1 and f_2 with equal probability.

As it was assumed that the amplitude of the external force is a random process, $\mathcal{F}_0$, the external force is also a random process and it is represented by $\mathcal{F}$. It is assumed that

$$\mathcal{F}(t) = \mathcal{F}_0(t)\ \sin(\omega_f\ t)\,, \tag{11}$$

where ω_f is a constant forcing frequency. Thus, $\mathcal{F}$ is a random process harmonic by parts.

6 SIMULATIONS OF THE STOCHASTIC SYSTEM

To make the stochastic analysis of the nonlinear absorber, Monte Carlo simulations were employed to compute statistics of the response of the stochastic system. In the simulations, eq. 6, was integrated in a range of [0.0, t_f] seconds considering that each coordinate x_1, x_2 and x_3 has null initial conditions to position and to velocity. For the integrations, it was used the function *ode45* (based on the Runge-Kutta 4th/5th-order method with a varying time-step algorithm) of the *Matlab* software with a maximal steep size equal to 10^{-4} seconds. Also, the maximal absolute error allowed in the integrations was 10^{-4}.

The value of the time-interval T was fixed as 1.0 [s], in a way that in each simulation, one realization of $\mathcal{F}_0$ can have up to t_f constant parts. The values used to f_1 and f_2 were respectively 1 [N] and 2 [N]. All the others system parameter's have the same values used in the deterministic simulations (see table 1).

As it was assumed that the external force is a random process, $\mathcal{F}$, the displacement of each degree of freedom are also random process represented by $\mathcal{X}_1$ and $\mathcal{X}_2$. Its maximum displacements are random variables, noted as $X_1^\star$ and $X_2^\star$. Statistics of them, as mean ($\mu_{X_1^\star}$, $\mu_{X_2^\star}$) and standard deviation($\sigma_{X_1^\star}$, $\sigma_{X_2^\star}$), were computed for different values of the forcing frequency, ω_f, and of the nonlinear parameter γ.

For each value of γ and for a bandwidth of frequencies ω_f, the maximum values of $X_1^\star$ and $X_2^\star$ are random variables, noted as $X_1^{\star\star}$ and $X_2^{\star\star}$.

As done in the deterministic simulations, we start observing the response in time of the displacement of each degree of freedom when the forcing frequency, ω_f, is the same as the natural frequencies ω_1 and ω_2. Figures 18 and 19 show the envelope graphs of $\mathcal{X}_1$ and $\mathcal{X}_2$ constructed with 200 realizations of these random process for the system with and without the nonlinear absorber. By these figures, it is possible to verify that the nonlinear absorber reduces the mean of the amplitude of oscillation of both degrees of freedom simultaneously.

By the deterministic simulations, presented in section 4, it was possible to verify that the nonlinear absorber can reduce the amplitudes of oscillation for a harmonic force in a bandwidth of frequencies. To verify if the absorber has the same capability when the external force is stochastic, modeled as a random process harmonic by parts, the stochastic system with and without the nonlinear absorber was excited with different ω_f.

For each frequency, Monte Carlo simulations were employed to compute statistics of $X_1^\star$ and $X_2^\star$. Figures 20 and 21 show the mean and 90% confidence interval of $X_1^\star$ and $X_2^\star$ for forcing frequencies in the bandwidth [0.4, 12] [Hz]. For each frequency, these statistics were computed

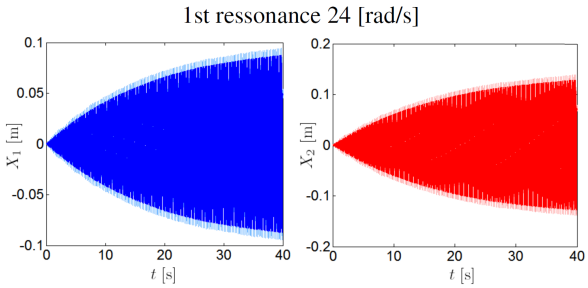

Figure 18: System without nonlinear absorber: mean and 90% confidence interval of $\mathcal{X}_1$ and $\mathcal{X}_2$ with $w_f = \omega_1$ and $w_f = \omega_2$ for $\gamma = 3 \times 10^3$ [1/(sm)^2].

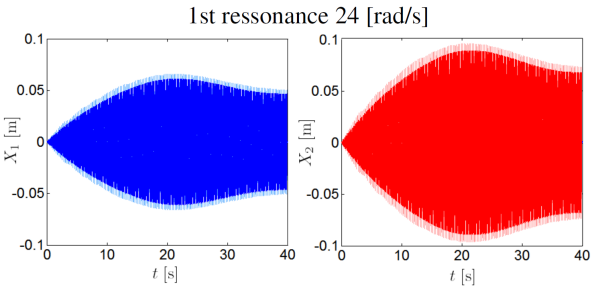

Figure 19: System with nonlinear absorber: mean and 90% confidence interval of $\mathcal{X}_1$ and $\mathcal{X}_2$ with $w_f = \omega_1$ and $w_f = \omega_2$ for $\gamma = 3 \times 10^3$ [1/(sm)^2].

with 100 realizations of the random process $\mathcal{F}$. In both graphs, the dotted black lines represent the mean of $X_1^\star$ and $X_2^\star$ of the stochastic system without the nonlinear absorber.

Comparing, for both degree of freedom, the means of the maximum displacement without and with the nonlinear absorber, it is possible to verify that the coupling of the absorber do not reduce the amplitude of oscillation in all bandwidth frequency. It reduces just for values of ω_f around ω_1 (that is the first frequency of resonance of the linear system, that is, without the absorber).

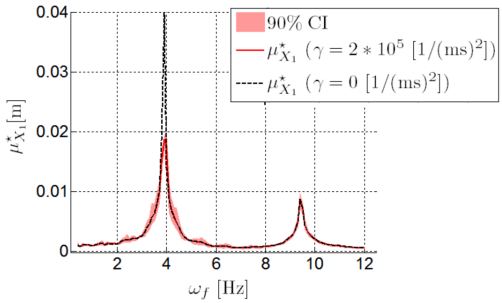

Figure 20: First degree of freedom: mean and 90% confidence interval of the maximum displacement of for forcing frequencies in bandwidth.

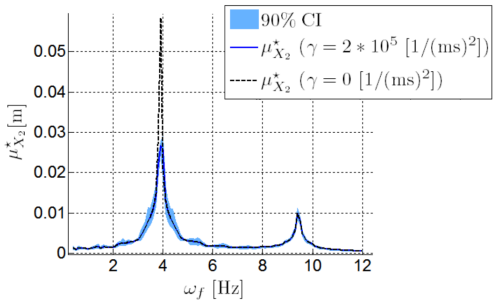

Figure 21: Second degree of freedom: mean and 90% confidence interval of the maximum displacement of the system of a bandwidth analysis.

To observe the influence of the parameter $\gamma = k_3/(m_3 l_a^2)$, eq. (5) in the reduction of the maximum displacements, for different values of this parameter, the system was excited with forcing frequencies, ω_f, in the bandwidth [0.4, 12] [Hz]. For each value of γ and ω_f, Monte Carlo simulations were employed to compute 100 realizations of $X_1^\star$ and $X_2^\star$. For each value of γ and for each bandwidth of frequencies, the maximum values of the realizations of $X_1^\star$ and $X_2^\star$ were computed. They are realizations of the random variables $X_1^{\star\star}$ and $X_2^{\star\star}$.

The results, that is, statistics to $X_1^{\star\star}$ and $X_2^{\star\star}$ for different values of γ , are shown in fig. 22. It is possible to verify that high values of γ can reduce the mean of the maximum amplitude of oscillation of each degree of freedom up to 70% with γ around 4×10^5 [1/m^{2}s^2].

7 CONCLUDING REMARKS

The results presented in this paper are consistent of what it is expected of a nonlinear absorber. The constructed instrumented test rig proved to be an interesting instrument for the study of nonlinear absorbers. Cubic springs are known devices found in the literature, but as theoretical system and rarely one sees how to realize one in practice, here one way is shown.

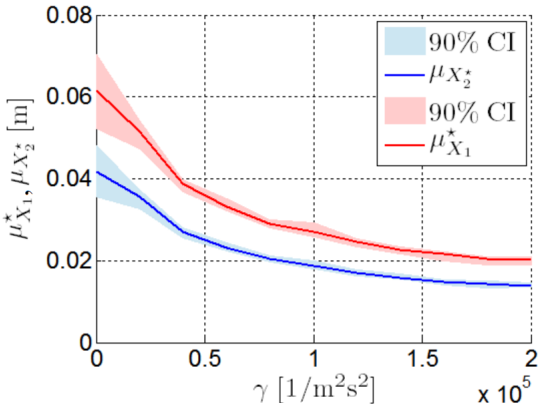

Figure 22: Mean and 90% confidence interval of $X_1^{\star\star}$ and $X_2^{\star\star}$ for different values of γ.

The present work proposes a way to built one nonlinear absorber with cubic characteristic and a test procedure of it in a test rig.

Experiments conducted with impact hammer and oscilloscope showed that a two-degree-of-freedom model is enough to simulate the behavior of a nonlinear absorber with a cubic relationship with the displacement. A concept of a real nonlinear absorber was presented, which would be described by governing equation for nonlinear absorber showed before. The concept would attach to the structure at the top and reduce the vibration on both platforms. The outcome of this experiment is still in process of analysis, also a better parameter estimation of the test rig and better instrumentation are part of future works.

In the deterministic analysis, the numerical simulations tested the influence of the nonlinear absorber for different forcing frequencies. It was confirmed the reduction of the maximum amplitude of oscillation of each degree of freedom not only at specific frequencies, but at all the bandwidth frequency tested, as shown in fig. 13. The sensibility of the system to the constant γ, which characterize the nonlinear absorber properties, was also examined. For different values of this parameter, the system was excited with forcing frequencies, ω_f, in the bandwidth [0.4, 12.0] [Hz] and the maximum obtained to $x_1^\star$ and $x_2^\star$ (noted as $x_1^{\star\star}$ and $x_2^{\star\star}$) were computed. It was shown that the amplitude of oscillation of the each degree of freedom were significantly reduced by increasing the value of γ, as observed in fig. 14 and 15. A reduction up to 50% to $x_1^{\star\star}$ and $x_2^{\star\star}$ was obtained with γ around 2.5×10^4 [1/m^{2}s^2].

In the stochastic analysis, it was assumed that the randomness is in the amplitude of the frequency force. It was modeled as a random process piecewise uniform, in a way that the external force is a random process harmonic by parts. Similar analyzes to those made previously to the deterministic system were developed, but in in this stage, in relation to the statistics of the random variables that characterize the response of the random system, that is $X_1^\star$, $X_2^\star$, $X_1^{\star\star}$ and $X_2^{\star\star}$.

The objective was to verify if the absorber when submitted to an stochastic force has the same capability of reduction that it has when is submitted to a harmonic force. Thus, the system with and without the nonlinear absorber was excited with a random force with different frequencies in the bandwidth [0.4, 12] [Hz]. Analyzing the results in term of the mean of $X_1^\star$ and $X_2^\star$, shown in fig. 20 and 21, it was possible to verify the absorber do not reduce the amplitude of oscillation at all bandwidth frequency. It reduces just for values of ω_f around ω_1 (that is the first frequency of resonance of the linear system, that is, without the absorber).

Comparing fig. 20 and 21 with fig. 14 and 15, one may note a huge difference between

the the maximum amplitude of oscillation of each degree of freedom. This happens because the amplitude of the excitation force in the deterministic simulations was considered to be 10.0 [N], while in the stochastic simulations it was much lower, 1.0 or 2.0 [N] depending on the instant and the realization of the random process $\mathcal{F}_0$.

The influence of the constant γ, which characterize the nonlinear absorber properties, was also observed in relation to the reduction of the mean of maximum displacements ($X_1^{\star\star}$ and $X_2^{\star\star}$), as shown in fig. 22. It was possible to verify that values of γ around 4×10^5 [1/m^{2}s^2] can reduce the mean of the maximum amplitude of oscillation of each degree of freedom up to 70%.

8 ACKNOWLEDGEMENTS

This work was supported by the Brazilian Agencies CNPQ, CAPES and FAPERJ.

REFERENCES

Bellizzi S..C.B. and Pinhede C. Vibration reduction using an attached local nonlinear passive absorber based on a clamped-clamped thin blade. *ASME 103 International Mechanical Engineering Congress & Exposition*, 2013.

Den Hartog J. *Mechanical Vibrations*. McGraw-HillBookCompany, NewYork, 4^{th} ed. edition, 1956.

Gendelman O. V. ; Starosvetsky Y. and Feldman M. Attractors of harmonically forced linear oscillator with attached nonlinear energy sink i: Description of response regimes. *Nonlinear Dynamics*, 51:31–46, 2008.

Inman D.J. *Engineering Vibration*. Prentice Hall Inc., Upper Saddle River, New Jersey, 3rd edition, 2007.

Kerschen G.; Vakakis A. F.; Lee Y.S.M.D.M.K.J.J. and Bergman L.A. Energy transfers in a system of two coupled oscillators with essential nonlinearity: 1:1 resonance manifold and transient bridging orbits. *Nonlinear Dynamics*, 42:283–303, 2005.

Kovacic I. and Brennan M.J. *The Duffing Equation: Nonlinear Oscillators and their Behaviour*. John Wiley & Sons, first edition edition, 2011.

S. K. and Høgsberg J. Tuned mass absorber on a flexible structure. *Journal of Sound and Vibration*, 333:1577–1595, 2014.

Starosvetsky Y. and Gendelman O. Vibration absorption in systems with a nonlinear energy sink: Nonlinear damping. *Journal of Sound and Vibration*, 324:916–939, 2009.

RESPONSIBILITY NOTICE

The authors are the only responsible for the printed material included in this paper.